J. Fluid Mech. (1979), *vol.* 90, *part* 1, *pp.* 21–32
Printed in Great Britain

Model studies of the closing behaviour of the aortic valve

By A. A. VAN STEENHOVEN AND M. E. H. VAN DONGEN

Departments of Mechanical Engineering and Physics,
Eindhoven University of Technology, The Netherlands

(Received 10 March 1978)

The closing mechanism of the natural aortic valve is investigated experimentally in a two-dimensional analogue. The interaction between the sinus content and the aortic flow when the latter is decelerating is studied for different Strouhal numbers: for high Strouhal numbers the sinus content rotates virtually as a rigid mass around the centre-line whereas for low Strouhal numbers, corresponding to the human situation, the cusp remains straight and slowly rotates around its point of attachment. Simple theoretical models based on the phenomena observed are proposed. Acceptable agreement between theory and experiment is found.

1. Introduction

The aortic valve is one of the four valves controlling the fluid motion through the heart. It is positioned at the outlet of the left ventricle, which pumps blood into the aorta. This valve is shown diagrammatically in figure 1. It has three leaflets (cusps) and behind each leaflet there is a cavity, the sinus of Valsalva. The leaflets are very thin (0·1–0·3 mm), non muscular and very flexible in the axial direction. The human left ventricle contracts and expands about once a second under normal conditions. The contraction phase of the left ventricle is called systole and the relaxation phase diastole. Figure 2 shows the blood flow in the aorta as a function of time; during the first part of systole there is an acceleration of the liquid, but when the pressure in the left ventricle starts decreasing, the liquid decelerates. At the very beginning of diastole there is a small reversed flow in the aorta. When the valve is closed, however, the velocity of the liquid in the aortic entrance is zero. During diastole the aortic valve has to withstand a mean pressure difference of about 80 mmHg.

The typical shape of the aortic valve and the role of the sinuses have attracted scientific interest for a long period starting with Leonardo da Vinci in 1513. Much more recently, it was Bellhouse & Talbot (1969) who recognized the important function of the sinus cavity in valve operation. From their model experiments, they observed that the closing of the valve has already started during the deceleration phase of the aortic flow, the valve being almost closed at the end of systole. A small reversed flow of about 2 % of the total forward flow then readily completes the closure. According to their observations, the ratio of the total reversed flow to the forward flow in the absence of the sinuses is about 25 %. The importance of this well-timed valve closure for the load on the valve leaflets was discussed by Spaan *et al.* (1975).

The shape of Valsalva's sinus was carefully examined by Reid (1970) and Swanson

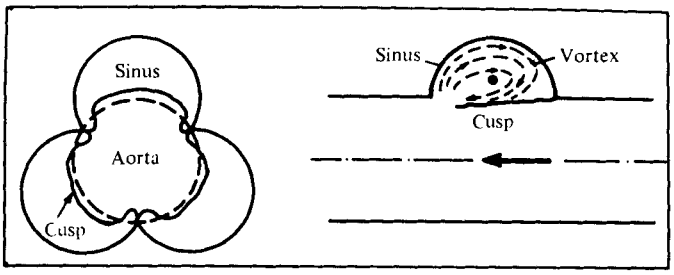

FIGURE 1. Diagram of the aortic valve and the sinus of Valsalva. (according to Bellhouse & Talbot).

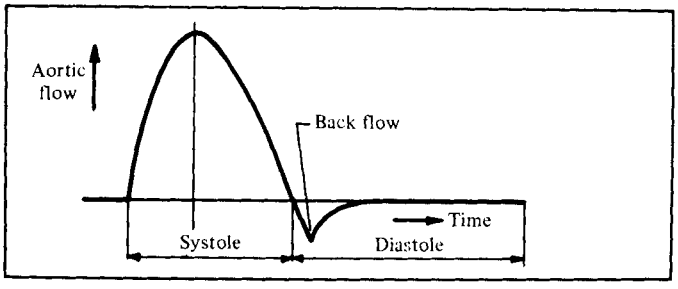

FIGURE 2. Diagram of the aortic flow as a function of time.

& Clark (1974). According to Reid, the sinus is a virtually hemispherical cavity with a radius equal to that of the aorta, the cusp length being about three-quarters of the sinus diameter. Swanson & Clark, however, concluded that the cavity height is about half the value reported by Reid.

Observations of the leaflet motion *in vivo* by means of high-speed cineangiograms were reported by Mercer (1973).

The fluid dynamics of the opening of the aortic valve have been investigated by Hung & Schuessler (1977). They studied the dynamic interaction of the leaflet motion with the accelerating aortic flow on the basis of an inviscid flow model. Gillani & Swanson (1976) presented a numerical solution of the Navier–Stokes equations for an accelerating flow field in an axisymmetric duct of variable axial geometry, representing the aorta and sinuses. They ignored the possible impedance of the valve leaflets on the flow. Viscous effects along the walls appear to play an important role and cause flow separation and the occurrence of primary and secondary vortices within the sinus cavity. The mechanism of the onset of valve closure during the deceleration of the main flow is not yet fully understood. Bellhouse & Talbot (1969) and Bellhouse (1969) suggested that the trapped vortex within the sinus interacts with the decelerating flow field and thus pushes the leaflets into the aorta. However, their description of this interaction is not entirely satisfactory; their model results in pressure differences across the cusps which seem to be quite large in view of the small mass of the leaflets.

In the present investigation attention is focused on the mechanism of valve closure as a result of flow deceleration. To that end, experiments were performed in a two-dimensional geometry. The aorta was represented by a channel of rectangular cross-section and the sinus, according to Reid (1970), by a half-cylinder, as shown in

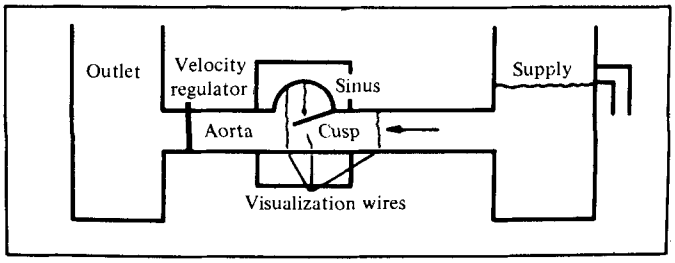

FIGURE 3. Diagram of the two-dimensional set-up of the aortic valve.

figure 3. The flow pattern and cusp motion were examined for various values of the rate of deceleration. Simple fluid-dynamical explanations based on the phenomena observed are proposed. The theory is also compared with the experimental results of Bellhouse & Talbot (1969). Finally the effect of sinus shape on valve operation is studied.

2. Two-dimensional model studies

Qualitative experimental observations

The two-dimensional model of the aortic valve has been designed as a rectangular duct with a half-cylindrical cavity in the upper wall, as shown in figure 3. The set-up has been described in more detail by van Steenhoven, van Dongen & Spaan (1976). A foil 2 μm thick (Makrofol KG) is used as the cusp material. The cusp length L is 1·5 times the sinus radius R. The flow is visualized by means of the hydrogen-bubble technique, as described by Merzkirch (1968, p. 39). The cathode is a thin (20 μm) platinum wire positioned in the flow field to be studied. The anode is a stainless-steel plate located in such a place that it does not disturb the flow. Hydrogen bubbles are produced periodically at the cathode by a square-wave generator. The flow in the two-dimensional model of the aortic valve is visualized at three different places: (i) in front of the aortic valve; (ii) just downstream the aortic valve; (iii) in the sinus. The experimental information is recorded on ciné film and still photographs. The test fluid is water and the channel has a fixed height of 4·5 cm and a width of 12 cm. The Reynolds number Re, defined as $U'h_0/\nu$, where U' denotes the maximum (initial) velocity of the mainstream, h_0 the channel height and ν the kinematic viscosity, can be varied between 2250 and 4500. The Reynolds number Re^* for the human aortic system, defined as $U'a/\nu$, where U' is the peak systolic velocity ($\sim$ 1 m/s), a the aortic radius ($\sim$ 1 cm) and ν the kinematic viscosity of blood ($\sim 3 \times 10^{-6}$ m^2 s^{-1}), has a value of the order of 4000 and lies within the experimental range attainable in the model. The mainstream can be decelerated at a constant rate from the value U' at $t = 0$ to zero at $t = \tau$. The Strouhal number St of the model flow, defined as $R/U'\tau$, R being the sinus radius, can be varied for a given U' by adjusting the deceleration time τ. In this way St can be varied between ∞ (stepwise velocity decrease) and 0·045. The Strouhal number St^* for the human aortic system, based on the sinus radius R ($\sim$ 1 cm), the peak systolic velocity U' and the time difference between maximum aortic flow and the onset of flow reversal at $t = \tau$ ($\sim$ 0·15 s), has a value of about 0·06.

The phenomena observed are strongly dependent on the Strouhal number. Figure 4 (plate 1) shows ciné pictures of the valve response to a practically stepwise velocity

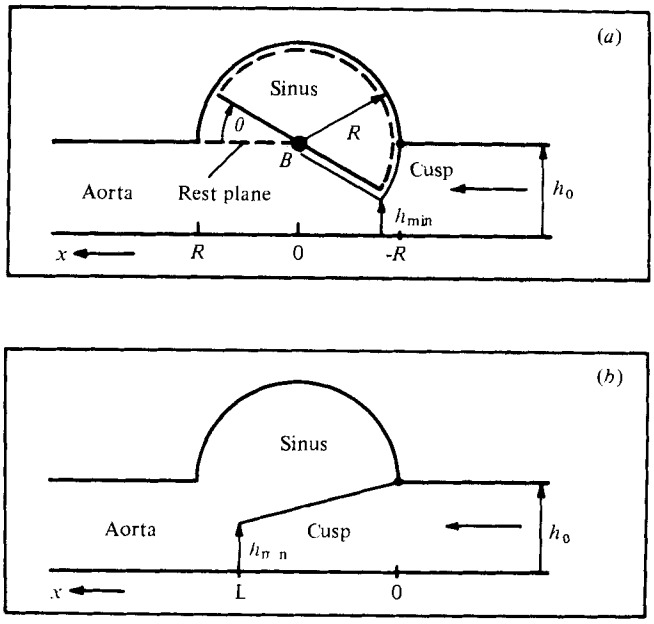

FIGURE 5. (a) Rigid-body rotation of the contents of the sinus for high Strouhal numbers. (b) Rotation of the leaflet around the point of attachment for low Strouhal numbers.

decrease. The contents of the cavity rotates almost like a rigid mass around line B in the separation plane of the sinus and aorta; see figure 5(a).

For low Strouhal numbers, $St < 0{\cdot}15$, the flow pattern is rather different as is shown in figure 6 (plate 2):

(i) The cusp moves slowly into the aorta, its shape does not change and it rotates around its point of attachment; see figure 5(b).

(ii) The velocity profile of the mainstream under the cusp remains virtually flat.

(iii) In the aorta at the rear of the cusp a region of recirculation is formed.

In all cases a vortex of moderate strength is present in the sinus cavity in the stationary situation. The maximum velocities observed in the sinus are about 15% of those in the mainstream. This is illustrated by figure 7 (plate 3).

Physical models

Since the phenomena observed depend on the Strouhal number we propose two different explanations based on observations and physical arguments, one for high Strouhal numbers ($St > 0{\cdot}3$) and the other for low Strouhal numbers ($St < 0{\cdot}15$).

High Strouhal numbers

At the beginning of the deceleration of the mainstream the cusp is practically parallel to the centre-line of the aorta (figure 5a) in a plane which will be referred to as the rest plane. Deceleration of the liquid in the aorta results in a pressure gradient in the axial direction such that the pressure increases downstream. The overall axial pressure gradient will generally cause a complicated fluid velocity distribution inside the cavity as well as in the adjacent part of the aorta. At a high Strouhal number the fluid

in the cavity performs a rigid-body-like rotation around an axis through the centre of the rest plane, pushing the cusp into the aorta.

In order to give a simplified description we represent the sinus fluid by a rotatable rigid half-cylinder with a specific mass ρ equal to that of the fluid. We also assume that the fluid motion in the aorta may be considered to be quasi-one-dimensional, which implies that both the pressure and the velocity are functions of the space co-ordinate x and time t only. The pressure and velocity just upstream of the entrance plane of the valve are denoted by $p_0(t)$ and $u_0(t)$. We now define a closing parameter λ as the ratio of the smallest height beneath the cusp to the height of the channel: $\lambda = h_{\min}/h_0$ (cf. figure 5*a*). Then the height of the aorta beneath the sinus fluid is a linear function of x; viz. $h = h_0[1 + (1-\lambda)x/R]$. We further assume that the velocity v in the transverse direction is much smaller than the axial velocity u, such that $v/u = O(1-\lambda)$ with $1-\lambda \ll 1$. In all equations terms of order $(1-\lambda)^2$ will be neglected.

From the continuity equation $\partial h/\partial t + \partial(hu)/\partial x = 0$ we then obtain for the average velocity in a cross-section

$$u(x,t) = u_0 - \tfrac{1}{2}\frac{(R^2-x^2)}{R}\frac{d\lambda}{dt} - u_0(1-\lambda)\frac{x}{R}. \tag{1}$$

The pressure is found from Bernoulli's equation:

$$p(x,t) = p_0 + \tfrac{1}{2}\rho u_0^2 - \tfrac{1}{2}\rho u^2 - \rho\frac{\partial}{\partial t}\int_{-R}^{x} u\,dx'. \tag{2}$$

Insertion of $u(x,t)$ from (1) into (2) yields an expression for the pressure distribution in terms of u_0, λ, du_0/dt and $d\lambda/dt$. The axial pressure distribution causes a torque to act on the contents of the sinus, resulting in rotation of the contents of the sinus according to

$$\int_{-R}^{+R} px\,dx = J\frac{d^2\theta}{dt^2}, \tag{3}$$

where J is the moment of inertia of the contents of the sinus. The angle θ, defined in figure 5(*a*), is related to λ to first order by

$$\theta = (h_0/R)(1-\lambda). \tag{4}$$

The moment of inertia of a homogeneous half-cylinder with respect to its axis of symmetry is

$$J = \tfrac{1}{4}\rho\pi R^4. \tag{5}$$

After combining (1)–(4) and neglecting all terms of order $(1-\lambda)^2$, we find the following differential equation relating the rotation of the contents of the sinus to the rate of change of the mainstream velocity:

$$\left[\frac{Jh_0}{\rho R} + \tfrac{4}{15}R^4\right]\frac{d^2\lambda}{dt^2} + \tfrac{2}{3}R^2(1-\lambda)\,u_0^2 = \tfrac{2}{3}R^3\frac{du_0}{dt}, \tag{6}$$

with initial conditions $\quad d\lambda/dt = 0, \quad \lambda = 1 \quad \text{at} \quad t = 0. \tag{7}$

For a stepwise change in velocity $u = U[1 - H(t)]$, $H(t)$ being the unit step function, the solution becomes

$$\lambda = 1 - \tfrac{2}{3}tU/[\tfrac{1}{4}\pi h_0 + \tfrac{4}{15}R]. \tag{8}$$

Then the closing rate $d\lambda/dt$ is constant and depends on both the sinus radius and the initial velocity.

It is questionable whether Bernoulli's equation in the form (2) is applicable to this specific case, since the assumption $v/u = O(1-\lambda)$ is then certainly not uniformly valid. This might affect the second inertia term corresponding to the aortic flow in (6). For a stepwise velocity change this leads to a somewhat different value of the denominator in (8).

Low Strouhal numbers

At a low Strouhal number, of the order of that for the human situation, we observed that the cusp remains virtually straight and rotates slowly around its point of attachment when the main flow is decelerating. The path lines of the flow downstream of the cusp remain almost straight, so that no strong transverse pressure gradients are present. Initially, in the steady case, the maximum velocity within the sinus is much smaller than that of the mainstream, and this situation persists during the first phase of deceleration. Since also the rate of change of the velocity within the sinus is much smaller than the deceleration du_0/dt in the channel, the function of the cavity is to keep the pressure differences small, thus reducing the adverse pressure gradient and consequently the deceleration beneath the cusp. This is made possible by the cusp motion.

We shall assume in our model that the cusp remains straight and is able to rotate around its point of attachment. The leaflet cannot withstand a pressure difference across it because of its negligible mass. However, by prescribing the leaflet shape, this condition cannot be locally imposed upon the cusp. Instead, we take the average pressure difference across the cusp to be equal to zero. The sinus pressure is assumed to be constant, in view of the arguments given above, and is put equal to the pressure at the cusp tip.

Considering the flow to be quasi-one-dimensional and again defining the closing parameter λ as $h_{\min}/h_0$ (cf. figure 5*b*), we obtain the following continuity equation for the flow beneath the cusp:

$$u(x,t) = \left[u_0 - \frac{1}{2}\frac{x^2}{L}\frac{d\lambda}{dt}\right] \Big/ \left[1-(1-\lambda)\frac{x}{L}\right]. \tag{9}$$

Assuming v/u to be of order $1-\lambda$ and neglecting terms of order $(1-\lambda)^2$, the Bernoulli equation takes the form

$$p(x,t) = p_0 + \tfrac{1}{2}\rho u_0^2 - \tfrac{1}{2}\rho u^2 - \rho \frac{\partial}{\partial t}\int_0^x u\,dx', \tag{10}$$

where u_0 and p_0 denote the velocity and pressure at the entrance plane of the valve at $x = 0$. Substituting the velocity given by (9) into (10), we obtain for the pressure distribution to first order

$$p(x,t) = p_0 + \tfrac{1}{6}\rho \frac{x^3}{L}\frac{d^2\lambda}{dt^2} + \rho u_0 \frac{x^2}{L}\frac{d\lambda}{dt} - \rho x \frac{du_0}{dt} - (1-\lambda)\left[\rho \frac{x}{L} u_0^2 + \tfrac{1}{2}\rho \frac{x^2}{L}\frac{du_0}{dt}\right] = 0. \tag{11}$$

By setting the mean pressure difference across the cusp equal to zero, i.e.

$$\overline{\Delta p} = \frac{1}{L}\int_0^L [p(x,t) - p(L,t)]\,dx = 0, \tag{12}$$

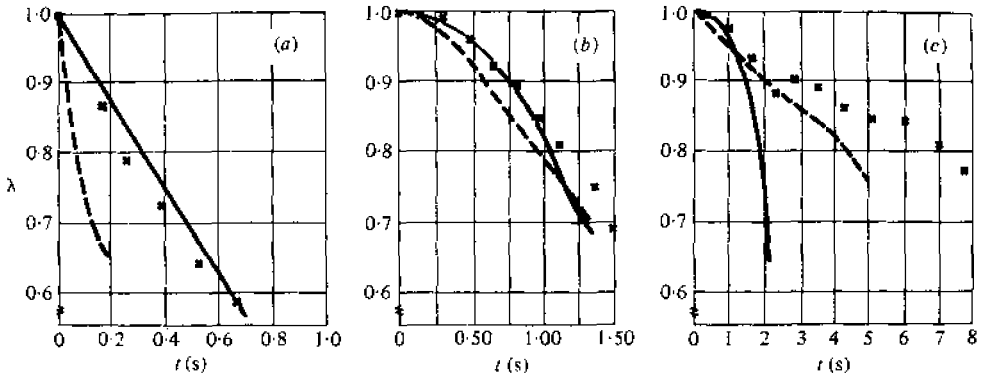

FIGURE 8. The closing behaviour at different Strouhal numbers ($R = 4{\cdot}5$ cm). ×, experiment; ——, model for high St; – – –, model for low St. (*a*) $St = \infty$, $U = 5$ cm/s, $\tau = 0$. (*b*) $St = 0{\cdot}2$, $U = 7$ cm/s, $\tau = 3$ s. (*c*) $St = 0{\cdot}06$, $U = 7$ cm/s, $\tau = 10$ s.

where the pressure in the sinus is taken equal to the pressure at the cusp edge, we finally arrive at a differential equation for λ of the form

$$\frac{d^2\lambda}{dt^2} + \frac{16}{3}\frac{u_0}{L}\frac{d\lambda}{dt} - (1-\lambda)\left[4\frac{u_0^2}{L^2} + \frac{8}{3}\frac{1}{L}\frac{du_0}{dt}\right] = 4\frac{1}{L}\frac{du_0}{dt} \tag{13}$$

with initial conditions $\quad d\lambda/dt = 0, \quad \lambda = 1 \quad \text{at} \quad t = 0.$

This equation describes the cusp motion as a function of time for small values of $1 - \lambda$ and for relatively low Strouhal numbers.

Comparison between theory and experiment

In order to compare theory and experiment, valve closure will be discussed for different Strouhal numbers and various values of the initial mainstream velocity and sinus radius.

Figure 8 shows the experimentally determined cusp displacement, characterized by λ, as a function of time for $St = \infty$, 0·2 and 0·06 for a Reynolds number of about 3300. On the basis of the velocity variation measured, (6) and (13), which correspond to the two different physical models, were solved numerically. For each experiment the calculated cusp displacement λ is also shown as a function of time in figure 8. For $St > 0{\cdot}3$ the contents of the sinus tends to rotate as a rigid mass into the aorta. The solution of (6), which is based upon this model of rigid rotation, shows fair quantitative agreement with the experiment. For $St < 0{\cdot}15$ it is (13), which is based upon the assumption of constant pressure on the sinus side of the cusp, that gives the best agreement with the experimental observations. For Strouhal numbers between these two different regions, a gradual transition in time is observed from the one model to the other. Initially a rigid-body rotation is observed. After a certain transition time the cusp becomes more and more stretched and the rotation centre moves from the sinus centre-line towards the point of attachment. For decreasing Strouhal numbers the transition time decreases and the initial rigid-rotation phase becomes of lessening importance.

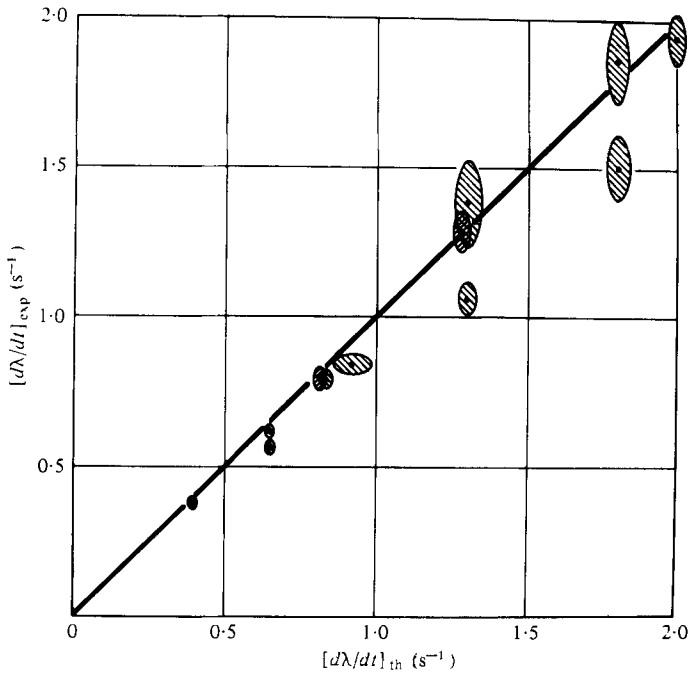

FIGURE 9. Relation between the theoretically predicted and the experimentally found closing rates after a stepwise decrease in the mainstream velocity. $St = \infty$, $U = 4$, 8 or 13 cm/s, $R = 3{\cdot}0$, $4{\cdot}0$, $4{\cdot}5$ or $5{\cdot}7$ cm, $\tau = 0$.

For Strouhal numbers of ∞ and 0·06, the velocity U and sinus radius R (thus the cusp length $L = \frac{3}{2}R$) were varied. The theoretical relation (6), which represents the physical model for high Strouhal numbers, was tested experimentally by observing the two-dimensional contents of the sinus after a stepwise change in the velocity of the mainstream. In these experiments four different radii and three different initial velocities were applied. The experiments indicate a linear relation between the closing parameter λ and time t which is in agreement with (8). For each combination of radius and initial velocity the measurements were repeated three or four times. By linear regression and variance analysis the experimental values for the slope of the linear relation between λ and t for different radii and initial velocities were determined. Figure 9 shows a comparison between these experimental values and the theory, together with the 95 % reliability interval. From this graph we may conclude that the agreement is fair.

The physical model for physiological values of the Strouhal number was tested experimentally for three different initial mainstream velocities and three different valve geometries. The results are shown in figures 10(*a*) and (*b*); each experimental point is the average result of four experiments; the inaccuracy $\Delta\lambda$, based on a 95 % reliability interval, is about 0·02. The cusp displacements as a function of time according to (13) are compared with the experimental results. The parametric dependence of the closing rate on the cusp length and initial mainstream velocity predicted by the model has indeed been observed experimentally. Theory and experiment show reasonable agreement for the range of parameters studied, particularly when it is realized that the assumptions concerning the pressure on the sinus side of the cusp are highly simplified.

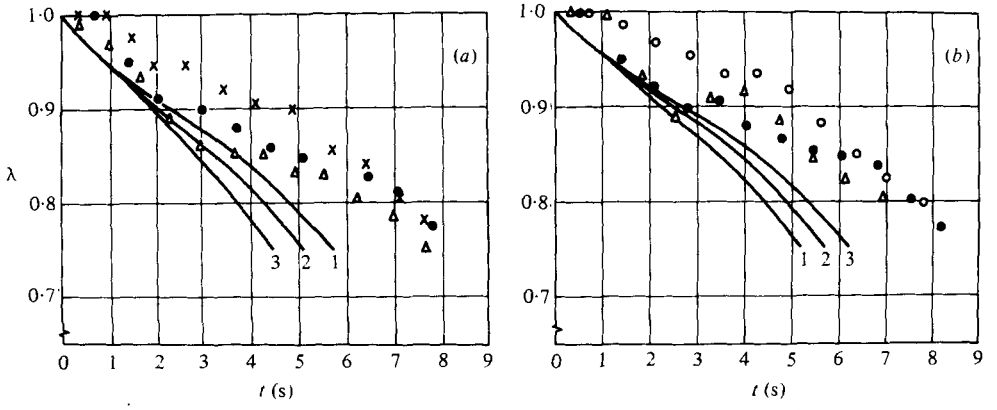

FIGURE 10. The closing behaviour at a Strouhal number in the low Strouhal number range for (*a*) different values of the initial mainstream velocity U and (*b*) different valve geometries (sinus radius R, annex cusp length L).

	Expt	Theory	U(cm/s)	St
(*a*)	×	——1	9	0·05
	●	——2	7	0·06
	△	——3	5	0·09

$R = 4{\cdot}5$ cm, $\tau = 10$ s

	Expt	Theory	R(cm)	L(cm)	St
(*b*)	●	——1	4·5	6·76	0·06
	△	——2	3·75	5·63	0·05
	○	——3	3·0	4·5	0·04

$U = 7$ cm/s, $\tau = 10$ s

3. Application of the model to the simulation experiments of Bellhouse and Talbot

Bellhouse & Talbot (1969) and Bellhouse (1969) reported on experiments with a three-dimensional analogue of a valve with an aortic diameter of 2·5 cm, which is about the size of a human aorta. The valve house was made of Perspex; the cusp material was 0·1 mm thick nylon. They tested their valve system in a pulsatile flow and measured the valve opening area A as a function of time. The measured flow velocity in the model aorta after the onset of deceleration ($t = 0$) could be well described by a quadratic function of time: $u_0(t) = U[1-(t/\tau)^2]$. Their experimental results are shown as open circles in figure 11.

In order to compare these experimental results with the low Strouhal number model, we have to extend the model to this three-dimensional situation. We assume that the cusps are arranged such that they together form a truncated cone. Then under the same assumptions as were made earlier for the two-dimensional case, we find for the present axisymmetric system, defining $\lambda^2 = A(t)/A(0)$, the following equation:

$$\frac{d^2\lambda}{dt^2}+\frac{16}{3}\frac{u_0}{L}\frac{d\lambda}{dt}-(1-\lambda)\left[4\frac{u_0^2}{L^2}+\frac{8}{3}\frac{1}{L}\frac{du_0}{dt}\right]=2\frac{1}{L}\frac{du_0}{dt}, \tag{14}$$

with initial conditions $d\lambda/dt = 0$, $\lambda = 1$ at $t = 0$.

This equation was solved numerically for quadratic time dependence of the velocity. The theoretical result is shown as a solid curve in figure 11, and here also reasonable agreement is found.

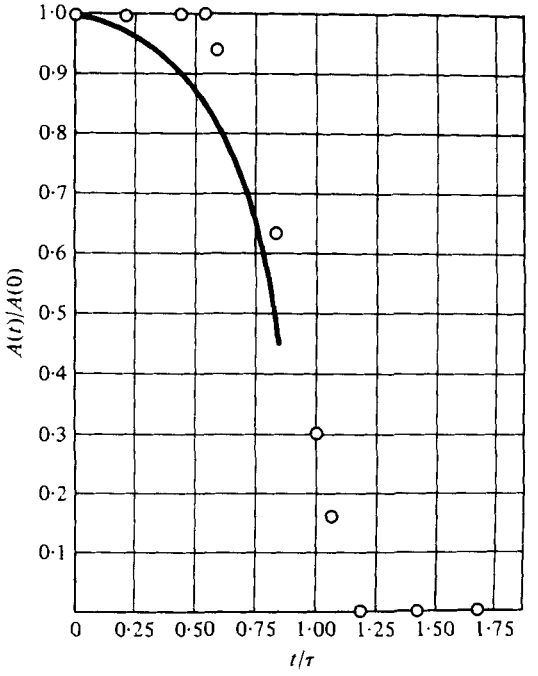

FIGURE 11. Comparison of the experimental results of Bellhouse (1969) with the present theory. ○, experiment; ——, theory. $St = 0{\cdot}13$, $U = 65\,\mathrm{cm/s}$, $R = 1{\cdot}25\,\mathrm{cm}$, $\tau = 0{\cdot}15\,\mathrm{s}$.

4. The influence of the shape of the sinus of Valsalva on valve closure

To study the role of the sinus of Valsalva in valve closure at the physiological value of the Strouhal number, two further series of experiments were performed in the two-dimensional analogue of the aortic valve. First, valve closure was investigated when the sinus cavity was partly deformed. This was done by filling the outer segment of the sinus with solid material. The rate of valve closure for different values of the sinus height is shown in figure 12(*a*). The sinus height can be reduced to less than half of its original value without a noticeable change in valve closure. However, the more the height of the cavity is reduced below this value, the more the closure is hampered.

In the second series the sinus radius R was changed, keeping the cusp length L constant. A larger ratio of sinus radius to cusp length than the physiological one appears to result in a faster closure, which also agrees better with the theory (figure 12*b*).

In both figures each experimental point has, analogously to figure 10, an inaccuracy of $\Delta\lambda = 0{\cdot}02$. The experimental observations show that for the mechanism of valve closure in the deceleration phase of systole the presence of a cavity of a certain minimum size is essential. Next, the experiment reveals that there is some freedom as to the shape of the cavity, and that some extension of the cavity in the axial direction may have a favourable effect on valve closure.

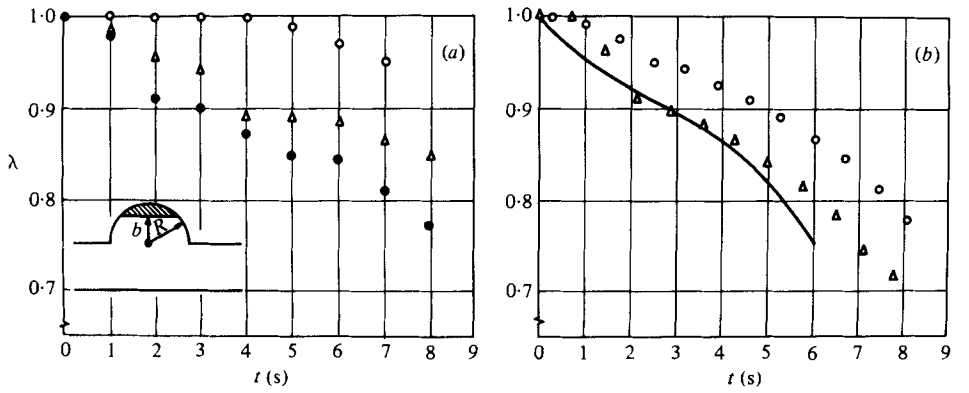

FIGURE 12. The influence of the sinus shape on valve closure ($U = 7$ cm/s, $\tau = 10$ s). (*a*) At different sinus heights b ($R = 4{\cdot}5$ cm). Experiment: ○, $b = 0$; △, $b = 0{\cdot}2R$; ●, $b = R$. (*b*) At different sinus radii R ($L = 4{\cdot}5$ cm). Experiment: ○, $R = 3{\cdot}0$ cm, $St = 0{\cdot}04$; △, $R = 4{\cdot}5$ cm, $St = 0{\cdot}06$. ——, theory.

5. Discussion

One of the main conclusions from the present experiments is that the flow phenomena and the cusp motion are strongly dependent on the Strouhal number. For physiological applications, the low Strouhal number experiments and analysis are the most important ones. A simplified quasi-one-dimensional description of the flow in the core beneath the cusp, combined with an assumption of constant pressure on the sinus side of the cusp, appears to give a good qualitative idea of the initial phase of valve closure.

The situation of a decelerating flow, starting from a steady state, is different from that of a pulsatile flow, in which the viscous forces along the wall and the leaflet may generate, during the acceleration of the fluid, a strong vortex which is trapped in the sinus cavity. This unsteady vortex is probably stronger than the steady one observed in the present experiments. The presence of such a strong vortex may cause a pressure distribution in the plane of the leaflet which is different from that under our experimental conditions. However, the fair agreement between the low Strouhal number model, based on the assumption of a constant pressure in the sinus cavity, and the experiments of Bellhouse & Talbot suggests that the presence of such a stronger trapped vortex does not essentially affect the mechanism of valve operation.

The shape of the sinus is not very critical. The disagreement between Swanson & Clark and Reid concerning the sinus geometry is therefore not very relevant for the mechanism of valve closure.

We wish to thank Prof. dr. P. C. Veenstra, Prof. dr. G. Vossers and Dr J. A. E. Spaan for their valuable comments, Mr N. A. L. Touwen for his computer assistance and Mr A. A. M. Wasser for his laboratory assistance. We also thank all those students who contributed to this project.

REFERENCES

BELLHOUSE, B. J. 1969 Velocity and pressure distributions in the aortic valve. *J. Fluid Mech.* **37**, 587.

BELLHOUSE, B. J. & TALBOT, L. 1969 The fluid mechanics of the aortic valve. *J. Fluid Mech.* **35**, 721.

GILLANI, N. V. & SWANSON, W. M. 1976 Time-dependent laminar incompressible flow through a spherical cavity. *J. Fluid Mech.* **78**, 99.

HUNG, T. K. & SCHUESSLER, G. B. 1977 An analysis of the hemodynamics of the opening of aortic valves. *J. Biomech.* **10**, 597.

MERCER, J. L. 1973 The movements of the dog's aortic valve studied by high-speed cine-angiography. *Brit. J. Radiol.* **46**, 344.

MERZKIRCH, W. 1968 *Flow Visualization.* Academic Press.

REID, K. 1970 The anatomy of the sinus of Valsalva. *Thorax* **26**, 79.

SPAAN, J. A. E., VAN STEENHOVEN, A. A., VAN DER SCHAAR, P. J., VAN DONGEN, M. E. H., SMULDERS, P. T. & LELIVELD, W. H. 1975 Hydrodynamical factors causing large mechanical tension peaks in leaflets of artificial triple leaflet valves. *Trans. Am. Soc. Artif. Int. Organs* **21**, 396.

STEENHOVEN, A. A. VAN, VAN DONGEN, M. E. H. & SPAAN, J. A. E. 1976 Two-dimensional model experiments on the closing of the aortic valve. *Trans. Europ. Soc. Artif. Organs* **3**, 127.

SWANSON, W. M. & CLARK, R. E. 1974 Dimensions and geometric relationships of the human aortic valve as a function of pressure. *Circ. Res.* **35**, 871.

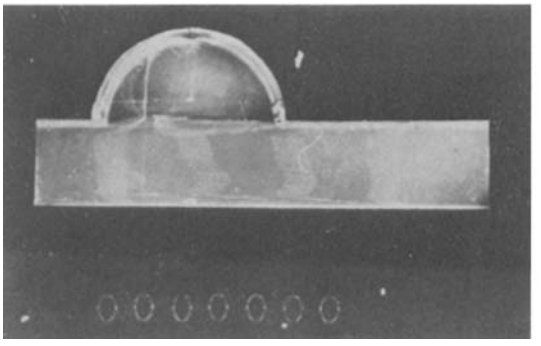

$t = 0$

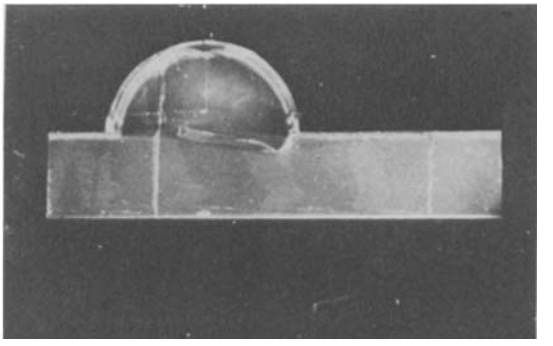

$t = 0{\cdot}36$s

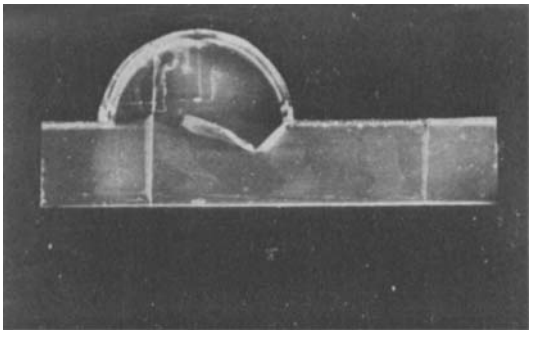

$t = 0{\cdot}75$s

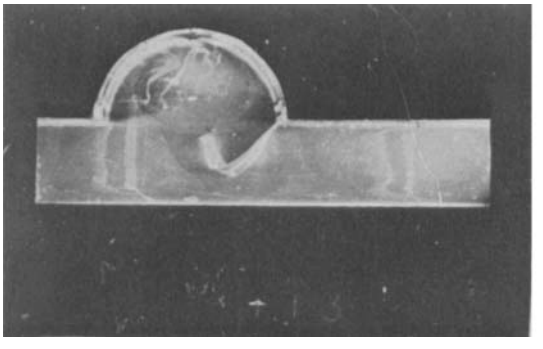

$t = 1{\cdot}13$s

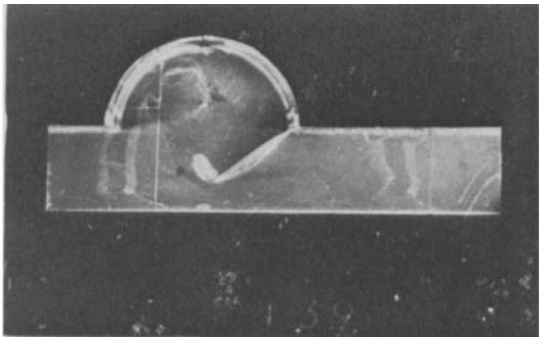

$t = 1{\cdot}39$s

FIGURE 4. Ciné pictures of the motion of the leaflet for a stepwise decrease in the mainstream velocity ($St = \infty$, $U = 5$ cm/s, $R = 4{\cdot}5$ cm, $\tau = 0$).

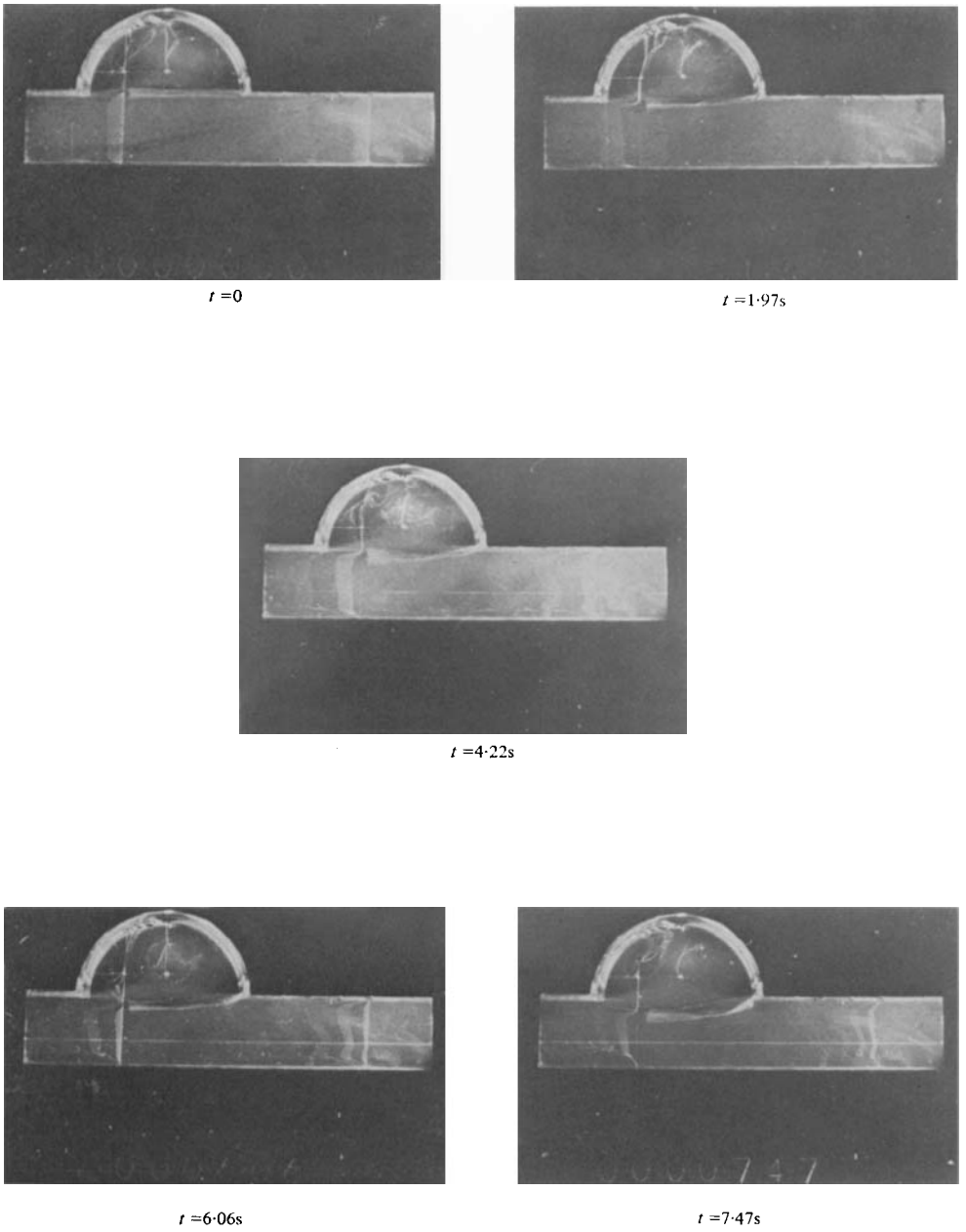

FIGURE 6. Ciné pictures of the motion of the leaflet for a gradual deceleration of the mainstream ($St = 0{\cdot}06$, $U = 7$ cm/s, $R = 4{\cdot}5$ cm, $\tau = 10$ s).

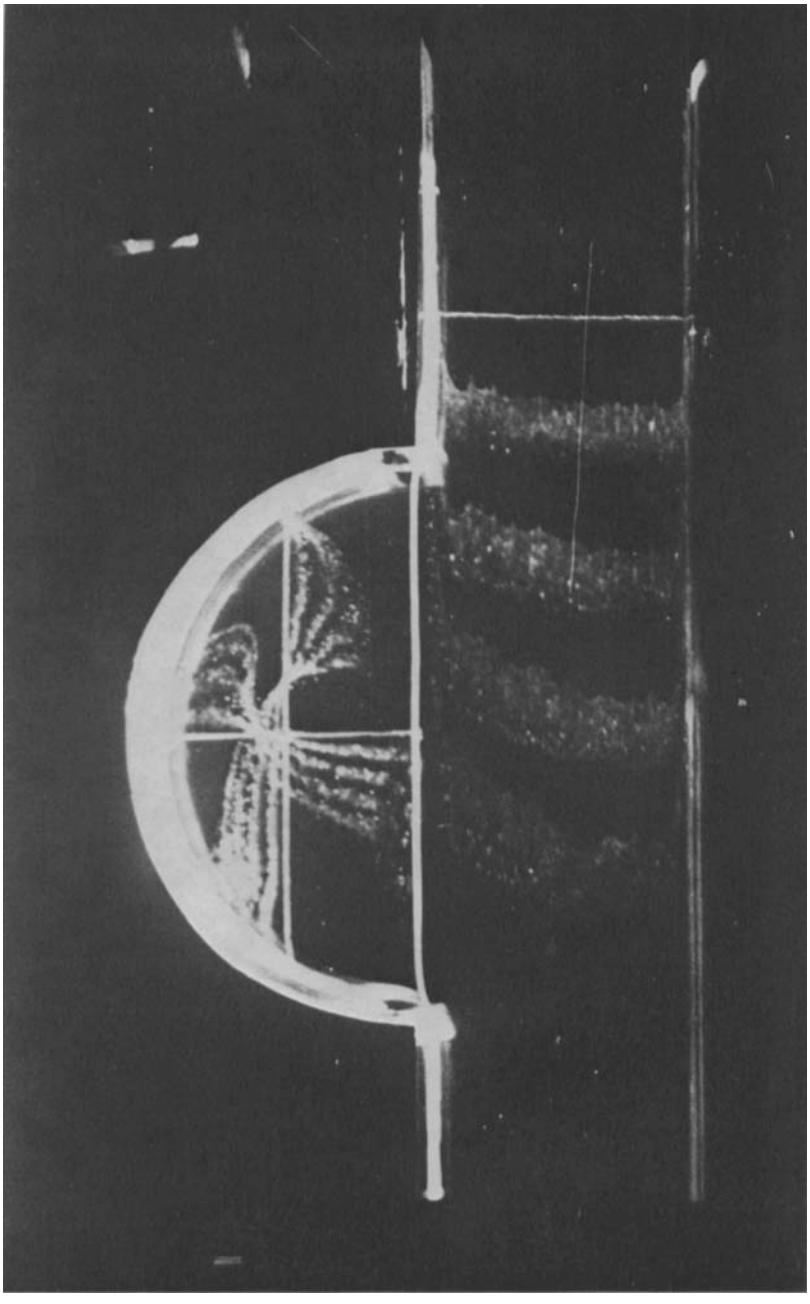

FIGURE 7. Ciné picture of the velocity distribution in the sinus and aorta in the stationary case without a cusp ($U = 3$ cm/s, $R = 4{\cdot}5$ cm).